IEEE Access
Multidisciplinary | Rapid Review | Open Access Journal

Received March 13, 2019, accepted March 29, 2019, date of publication April 9, 2019, date of current version May 7, 2019.

Digital Object Identifier 10.1109/ACCESS.2019.2909550

Dynamic Characteristic Optimization of Ball Screw Feed Drive in Machine Tool Based on Modal Extraction of State Space Model

YANG YONG[1], ZHANG WEI-MIN[2], ZHU QI-XIN[1], AND JIANG QUAN-SHENG[1]
[1]College of Mechanical Engineering, Suzhou University of Science and Technology, Suzhou 215009, China
[2]College of Mechanical Engineering, Tongji University, Shanghai 200092, China

Corresponding author: Yang Yong (yangyong5114360@163.com)

This work was supported in part by the Chinese National Natural Science Foundation under Grant 51805346, in part by the Chinese National Natural Science Foundation under Grant 51875380, in part by the National Science and Technology Major Project: High-grade Numerical Control Machine Tool and Basic Manufacturing Equipment under Grant 2012ZX04005031.

ABSTRACT The accurate prediction and research about the dynamic characteristic of machine tool during the design process are essential to develop high-performance machines. In order to consider the effect of mechanical modal characteristics on the whole dynamic performance and servo controller of ball screw feed drive fully, the modal characteristics of mechanical transmission are extracted and solved based on reduced state space matrix of ball screw feed system, which is also easy for integration with servo control model. On this basis, the step-by-step optimization method from the global to the local is proposed to optimize the servo controller and overall dynamic performance of ball screw feed drive. This step-by-step optimization method is as follows: first, the global initial optimal tuning of servo controller parameters under the influence of structure modal characteristics is originally realized through the analytic derivation of servo controller based on the extraction of state space modal characteristics. Second, the integrated model of the feed drive system is established. Finally, based on the above global optimization results, the overall dynamic performance, and the servo parameters of the feed drive system under the influence of the modal characteristics are further studied and optimized locally. Taking the ball screw feed drive studied in this paper like the example, its rise time and the settling time of step response are 0.089 and 0.104s before optimization, while these reduce to 0.038 and 0.092s after optimization. Its dynamic response performance after optimization is much better. The optimization result is also validated by the test: the rise time and the settling time by the test are 0.042 and 0.094s, which are close to that from the simulation. Also, the consistency of step response curves from experiment and simulation as well. All these show that: this prediction and optimization method of overall dynamic performance considering the modal characteristic influence of mechanical transmission fully is correct and reliable.

INDEX TERMS Ball screw feed drive in machine tool, dynamic characteristic, servo parameters, modal property, state space, step-by-step optimization method from the global to the local.

I. INTRODUCTION

Due to the strong competition in the market and the high requirements from the customers, the performance of machine tools has to be improved continuously. Time to market is shorter, while performance requirements are higher. Therefore, it is essential that: the dynamic characteristic of machine tool during the design process is predicted and researched accurately [1], [2].

The associate editor coordinating the review of this manuscript and approving it for publication was Hamid Mohammad-Sedighi.

The ball screw feed drive is commonly used in CNC machine tools because of its high stiffness, high transmission efficiency, low heating and wear resistance, etc. The ball screw feed drive system of machine tool is the typical electromechanical system. In this system, the servo control and mechanical transmission, which are closely linked, also interacted and influenced by each other, affect the dynamic performance of whole servo drive system together [3]–[5].

In fact, the frequency response performance of servo control system is affected by the vibration of

mechanical transmission. In order to avoid the instability of whole servo drive, the gain of position loop should be reduced. Due to that the natural frequency of feed system is much lower than the cutoff frequency of servo control loop itself, the control signal only in the control bandwidth lower than natural frequency can be transferred without delay and attenuation. So it can be concluded that: the frequency response of servo control system, and also the dynamic response performance of whole ball screw feed system are both influenced and restricted by the structure flexibility and modal characteristics greatly.

So the accurate prediction and optimization about dynamic performance of feed drive under the influence of structural flexibility and modal characteristics is essential to improve the accuracy and stability of whole ball screw feed drive.

The relative study about whole dynamic performance of ball screw feed drive, also the corresponding gaps are summarized and characterized as follows:

(1) By simplifying mechanical transmission system as the equivalent rigid body, the research of control algorithm (strategy) of servo controller and the whole ball screw feed system is more highlighted.

Although this method [6], [7] is easy to realize the integrated modeling of mechanical transmission system and servo control, the influence of flexibility, deformation and modal characteristics of mechanical structure on the servo control and the dynamic performance of whole feed drive system isn't considered too much.

(2) Based on the lumped parameter method, hybrid modeling method or derivation of Lagrange equation, etc., the dynamics model of ball screw feed system is established and then is integrated with the servo control in the same simulation environment, so as to research the control of whole servo drive under the influence of structure flexibility and modal characteristics.

The modeling based on lumped parameter method [8], [9] and formulation of Lagrange equation can effectively reduce the degree of freedom of model and also the order-number of transfer function [10], [11], and is helpful for the qualitative analysis of system and the estimation of vibration frequency. In addition, this modeling is also easy to integrate with servo control model. However, this modeling method, which is too simplified, restrains the important factors which affect the system performance, such as the structure flexibility, the joint stiffness, etc. Compared with the lumped mass method, the hybrid modeling method [8], [12], [13] is improved. However, the hybrid modeling method can't fully consider the influence of the structural flexibility (arising from flexible parts, joint region and so on) on the dynamic performance of the whole feed drive system also.

On the whole, this kind of research method is convenient to integrate modeling of mechanical transmission and servo drive. But it has some defects in the accurate analysis for modal and vibration characteristics of ball screw feeding system, and also in taking full consideration of influence from the mechanical structure flexibility and modal characteristics on the servo controller and the overall dynamic performance.

(3) The each sub modules of ball screw feed system are modeled in different simulation environments, and then the coupling modeling and integration of whole servo feed drive system is realized through the transfer of interface information in the simulation process.

In this method, the integrated modeling and dynamic performance of the ball screw feed drive system are realized by the interactive interface of simulation software [14]–[16]. However, the standard and expansibility of software interface still need to be further improved. In addition, the influence of structure flexibility and vibration of mechanical transmission on the overall dynamic performance and servo controller isn't also considered fully. Moreover, with the increase of number of flexible modeling components in the model, the computation efficiency and speed is reduced significantly.

(4) Additionally, some researches use the FEM (finite element method) for the dynamic modeling of mechanical transmission of ball screw feed system.

Though it can accurately describe the vibration and modal characteristics of machine tool, the overall dynamic model based on this method is complex and the number of degrees of freedom is numerous [17]–[19]. Obviously, it is not easy to integrate with control system model, so as to research the servo controller and the whole dynamic performance of feed drive system under the influence of structure flexibility and mode characteristics.

As far as the optimization of servo parameters and dynamic performance of ball screw feed drive system is concerned, the relative study and the corresponding gaps are summarized and characterized as follows:

(1) The self-tuning method based on analysis of approximate model.

In this method, the optimal values of servo parameters are determined through the analysis of tuning rules, which is relatively simple [20], [21]. It is relative simple. But the mechanical transmission is always simplified into one equivalent rigid body so as to integrate with servo control model conveniently, which pays less attention to the influence from structural flexibility and modal vibration. It could easily lead to that the servo parameters derived finally may not be the optimal because of the simplistic rigid model and the less focus on the structural flexibility influence.

(2) The self-tuning method based on optimization rules. With the help of intelligent optimization algorithm [22], [23], the optimization of control parameters is realized in this method.

Its optimization effect is better than the former. However, in the cascade control loop often used by traditional servo control system, the inclusion relationship exists in the current loop, velocity loop, and position loop which shows the obvious nonlinear characteristics. Also the control parameters with different scales of magnitude exist in the same mathematical model. All these lead to that: the control parameters are sensitive to the initial value of optimization, the

optimization result of control parameter is easy to fall into local optimal value, etc. Generally the optimization process often needs the given interval and initial value of optimization variables. Therefore, this method puts forward higher requirements for the accurate initial value close to the optimal value. But in the method, the interval and initial value of variables are often defined by experience, and the definition of optimizing interval and initial value of variables is inaccurate. Also in order to avoid the omission of the optimal value, a larger definition of the optimal interval is often used. All these are bad to the reliability of the final optimization.

The proposed prediction and optimization method of overall dynamic performance of ball screw feed drive based on modal extraction of state space model in this paper is characterized as follows:

Aiming at the above problems, the influences of modal characteristics and structure flexibility on the whole dynamic performance and servo controller of feed drive are fully considered in this paper, so as to accurately predict and research the dynamic performance and the servo controller of feed drive.

Above all, based on the reduced state space matrix of ball screw feed system, the modal characteristics of mechanical transmission are solved and extracted, which is also easy to be integrated with the servo control system. **(in Section 2)**

Then, on the above basis, the step-by-step optimization method from the global to the local instead of the traditional single-step optimization method is proposed, so as to optimize the servo controller and whole dynamic performance under the influence of structure flexibility and modal characteristics, which can overcome the problems mentioned above. This step-by-step optimization method **(in Section 3)** is as follows:

Firstly, through the analytic derivation of servo controller based on the extraction of state space modal characteristics, the global initial optimal tuning of servo controller parameters under the influence of modal characteristics is carried out. **(in Section 3.1).** And it includes:

Originally, the optimization estimations of gain and delay time of speed loop are realized by synthesizing the complex ratio method with the extraction of state space modal characteristics. **(in Section 3.1.1).**

Also originally, the constrain relational equation of gain of position loop considering modal characteristics and structure flexibility is derived. And then the optimization estimation of gain of position loop is completed by solving this constrain relation equation based on the recurrence method. **(in Section 3.1.2).**

Secondly, the integrated model of feed drive system is established. Furthermore, by taking the optimal calculated result of servo controller parameters above as the initial value, based on the optimization algorithm, the overall dynamic performance and the servo controller under the influence of modal characteristics of system are farther studied locally. **(in Section 3.2)**

From the above process, we can see that this proposed optimization method includes: (1) initial global estimation, i.e. global optimization: the initial estimation by analytic derivation of servo controller based on the extraction of state space modal characteristics considering the influence of modal characteristics. (2) Further local exact optimization: based on the initial optimal calculated result of servo controller parameters above, overall dynamic performance and the servo controller under the influence of modal characteristics of system are farther optimized exactly and locally.

Compared to the self-tuning method based on the analysis of approximate model, this proposed method introduces the reduced state space model based on the multi-flexible-body, and involves more influence from the structure flexibility and mode characteristics. Obviously, this method with more consideration of structure flexibility is more in line with the actual situation. Furthermore, the initial global analytic estimate is further refined optimally instead of taking this analytic value as the finally optimal result, so as to improve the reliability of the final optimization. Compared to the self-tuning method based on optimization rules, the optimal servo parameters considering modal characteristics are taken as initial values to further optimize in this proposed method instead of the values from experience. The more accurate definition of initial value is beneficial to the reliability of the final optimization.

When comparing these methods to illustrate the advantages of the proposed method, traditional optimization method such as interior point method, Nelder-Mead method, etc., widely used in servo response optimization process, can be chosen as the representative. Because these optimization methods, always integrated in optimization tools, are more flexible for machine tool designers, who are not familiar with optimization algorithms and programming.

Based on the proposed method, in the design stage, the dynamic performance and the best motion response characteristics of ball screw feed system can be accurately predicted and determined, which can save the time and re-prototyping cost in the whole product development cycle, and is essential to develop the high performance machines and reduce the time to market.

II. MODAL CHARACTERISTICS EXTRACTION OF BALL SCREW FEED SYSTEM BASED ON REDUCED STATE SPACE MODEL

A. METHOD FOR MODAL CHARACTERISTICS EXTRACTION BASED ON REDUCED STATE SPACE MODEL

The general equation of structure dynamics of ball screw feed system can be written as

$$\boldsymbol{M}\,\ddot{\boldsymbol{x}}(t) + \boldsymbol{C}\,\dot{\boldsymbol{x}}(t) + \boldsymbol{K}\,\boldsymbol{x}(t) = \boldsymbol{Q}(t) \tag{1}$$

where $\boldsymbol{x}$ is the displacement vector of ball screw feed system, $\dot{\boldsymbol{x}}$ represents the speed vector, $\ddot{\boldsymbol{x}}$ refers to the acceleration vector, $\boldsymbol{M}$, $\boldsymbol{C}$ and $\boldsymbol{K}$ are mass matrix, damping matrix and stiffness matrix respectively, $\boldsymbol{Q}$ is the load vector. It is assumed that the n order natural frequency matrix and mode

shape matrix of system are $\boldsymbol{\Phi}$ and $\boldsymbol{\Omega}$ respectively, and also $\boldsymbol{\Phi} = [\boldsymbol{\varphi}_1, \boldsymbol{\varphi}_2 \ldots \boldsymbol{\varphi}_n]$, $\boldsymbol{\Omega} = \mathrm{diag}(\omega_1, \omega_2 \ldots, \omega_n)$, where $\boldsymbol{\varphi}$ is mode shape vector and ω is system circular frequency. Based on the basic principle of modal synthesis theory [24], [25], the motion vector $\boldsymbol{x}$ in the physical coordinates, can be approximately represented with the superposition of mode shape vector $\boldsymbol{\Phi}$ by taking the first m ($m \leq n$) orders modal principal coordinate $\boldsymbol{p}$ as the corresponding weighted coefficient. It can be expressed in matrix form as follows:

$$\boldsymbol{x} = \boldsymbol{\Phi}_{n\times m}\boldsymbol{p}_{m\times 1} \tag{2}$$

where the subscript $n \times m$ and $m \times 1$ represent the amount of row and column. By substituting Eq. (2) into the dynamic equation of ball screw feed system (Eq. (1)), and then by premultiplying $\boldsymbol{\Phi}^T_{m\times n}$, it can be obtained that:

$$\boldsymbol{M}_{m\times m}\ddot{\boldsymbol{p}}_{m\times 1} + \boldsymbol{C}_{m\times m}\dot{\boldsymbol{p}}_{m\times 1} + \boldsymbol{K}_{m\times m}\boldsymbol{p}_{m\times 1} = \boldsymbol{Q}_{m\times 1} \tag{3}$$

where $\boldsymbol{M}_{m\times m} = \boldsymbol{\Phi}^T_{m\times n}\boldsymbol{M}\boldsymbol{\Phi}_{n\times m}$, $\boldsymbol{C}_{m\times m} = \boldsymbol{\Phi}^T_{m\times n}\boldsymbol{C}\boldsymbol{\Phi}_{n\times m}$, $K_{m\times m} = \boldsymbol{\Phi}^T_{m\times n}\boldsymbol{K}\boldsymbol{\Phi}_{n\times m}$, $\boldsymbol{Q}_{m\times 1} = \boldsymbol{\Phi}^T_{m\times n}\boldsymbol{Q}$. It can be seen that: by modal coordinate transformation and modal synthesis method, the reduced dynamics model of ball screw feed system expressed in modal coordinates is obtained, as shown in Eq. (3). By setting that $\boldsymbol{p}_1 = \boldsymbol{p}_{m\times 1}$ and $\boldsymbol{p}_2 = \dot{\boldsymbol{p}}_{m\times 1}$, the equation $\dot{\boldsymbol{p}}_1 = \boldsymbol{p}_2$ can be obtained. By substituting $\boldsymbol{p}_1 = \boldsymbol{p}_{m\times 1}$ and $\boldsymbol{p}_2 = \dot{\boldsymbol{p}}_{m\times 1}$ into Eq. (3), and then by premultiplying $\boldsymbol{M}^{-1}_{m\times m}$, it can be got as follows:

$$\dot{\boldsymbol{p}}_2 = \boldsymbol{M}^{-1}_{m\times m}\boldsymbol{Q}_{m\times 1} - \boldsymbol{M}^{-1}_{m\times m}\boldsymbol{C}_{m\times m}\boldsymbol{p}_2 - \boldsymbol{M}^{-1}_{m\times m}\boldsymbol{K}_{m\times m}\boldsymbol{p}_1 \tag{4}$$

By setting that $\dot{\boldsymbol{X}} = [\dot{\boldsymbol{p}}_1, \dot{\boldsymbol{p}}_2]^T$, the following matrix form can be derived:

$$\dot{\boldsymbol{X}} = \begin{bmatrix}\dot{\boldsymbol{p}}_1\\ \dot{\boldsymbol{p}}_2\end{bmatrix} = \begin{bmatrix}0 & \boldsymbol{I}\\ -\boldsymbol{M}^{-1}_{m\times m}\boldsymbol{K}_{m\times m} & -\boldsymbol{M}^{-1}_{m\times m}\boldsymbol{C}_{m\times m}\end{bmatrix}\begin{bmatrix}\boldsymbol{p}_1\\ \boldsymbol{p}_2\end{bmatrix} + \begin{bmatrix}0\\ \boldsymbol{M}^{-1}_{m\times m}\end{bmatrix}\boldsymbol{Q}_{m\times 1} \tag{5}$$

where $\boldsymbol{I}$ is the unit matrix. By setting that $\boldsymbol{Y} = \boldsymbol{p}_1 = \boldsymbol{p}_{m\times 1}$, its matrix form can be shown as:

$$\boldsymbol{Y} = \begin{bmatrix}1 & 0\end{bmatrix}\begin{bmatrix}\boldsymbol{p}_1\\ \boldsymbol{p}_2\end{bmatrix} \tag{6}$$

By combing Eq. (5) and (6),reduced state space equation of ball screw feed system can be obtained:

$$\begin{cases}\dot{\boldsymbol{X}} = \boldsymbol{A}\boldsymbol{X} + \boldsymbol{B}\boldsymbol{u}\\ \boldsymbol{Y} = \boldsymbol{C}\boldsymbol{X} + \boldsymbol{D}\boldsymbol{u}\end{cases} \tag{7}$$

where

$$\boldsymbol{A} = \begin{bmatrix}0 & \boldsymbol{I}\\ -\boldsymbol{M}^{-1}_{m\times m}\boldsymbol{K}_{m\times m} & -\boldsymbol{M}^{-1}_{m\times m}\boldsymbol{C}_{m\times m}\end{bmatrix},$$
$$\boldsymbol{B} = \begin{bmatrix}0\\ \boldsymbol{M}^{-1}_{m\times m}\end{bmatrix}, \quad \boldsymbol{C} = \begin{bmatrix}1 & 0\end{bmatrix},$$
$$\boldsymbol{D} = 0, \quad \boldsymbol{X} = \begin{bmatrix}\boldsymbol{p}_1\\ \boldsymbol{p}_2\end{bmatrix}, \ \boldsymbol{u} = \boldsymbol{Q}_{m\times 1}.$$

In Eq. (7), $\boldsymbol{u}$ represents the force, which is the input; and $\boldsymbol{Y}(\boldsymbol{p}_{m\times 1})$ represents the movement response under modal coordinate, which is the output. Through the above reduced state space equation, the solution of motion response $\boldsymbol{x}$ in physical coordinates is transformed into the solution of motion response $\boldsymbol{p}_{m\times 1}$ in modal coordinates.

After the solution of motion response $\boldsymbol{p}_{m\times 1}$ in modal coordinates, the motion response $\boldsymbol{x}$ in physical coordinates can be achieved by Eq. (2), i.e. $\boldsymbol{x} = \boldsymbol{\Phi}_{n\times m}\boldsymbol{p}_{m\times 1}$.

According to the structural vibration principle [24], [36], the influence of low-order modal modes on structural vibration is greater. The energy proportion of high-order modal modes is lower, and their effect on the structure vibration is weaker. The structural vibration mainly depends on low-order modes. Therefore, the low-order modal modes are selected for the construction of reduced state space model. The motion response error caused by modal-mode truncation mainly depends on whether the excitation-force can excite the vibration generated by abandoned high-order modal-modes [24], [36].

On the one hand, the determination of low-order modal-modes for reduced state space modeling needs engineering experience. On the other hand, the selection of low-order modal-modes can be attempted repeatedly. If the motion response solution accuracy of reduced state space model is poor, the number of modal-modes can be further increased.

The determination of low-order modal-modes can be achieved according to the concerned frequency response bandwidth of excitation. Generally, the determination rule [24], [36] is: the maximum mode frequency of selected modal-modes should be about twice the concerned frequency bandwidth, at least greater than the concerned frequency bandwidth. If the response solution accuracy of reduced state space model is poor through the above rule, the number of modal can be further increased.

In order to fully consider the influence of structural flexibility, the multiple-flexible-body dynamic model of the ball screw feed system expressed by Eq. (1) is constructed by the finite element method. Based on the FE multiple-flexible-body dynamic model of ball screw system, the coefficient matrix and mode shape matrix (In Eq. (7)) of structural dynamic model of ball screw feed system can be obtained with the help of FE software and the corresponding modal analysis. Through MATLAB, by substituting these coefficient matrixes and mode shape matrixes into the Eq. (7), the reduced state space model of ball screw feed system can be obtained finally. On the one hand, this reduced state space model of ball screw feed system is easy to integrate modeling with the servo control; on the other hand, it can accurately solve the motion response performance under the influence of modal characteristics. And this schematic diagram of the modeling is shown in Fig. 1. Its state space equation can be solved by MATLAB to achieve the motion response solution.

B. MODAL CHARACTERISTICS EXTRACTION OF THE BALL SCREW FEED SYSTEM STUDIED IN THIS PAPER

The finite element model of the ball screw feed system is shown in Fig. 2(a). The column, machine tool bed, ram and

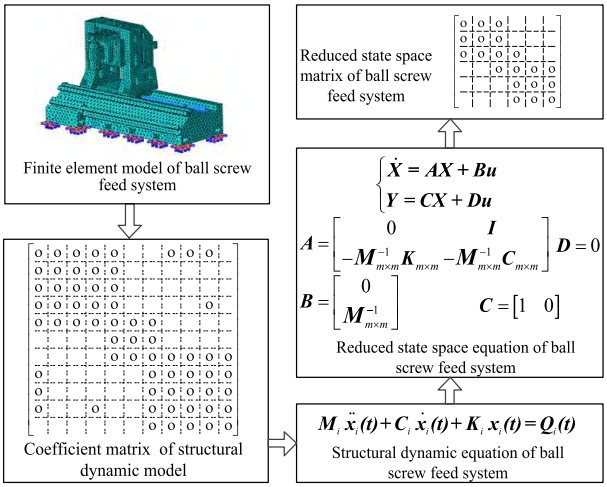

FIGURE 1. Process chart of reduced state space modeling of ball screw feed system.

so on are modeled by modified 3D solid elements, which can effectively overcome the problem of shear locking of element, and also ensure the solution accuracy. The motor shaft and screw shaft are modeled by beam element with cross section.

In addition, the material of column, ram, bed and etc. are cast iron, whose density, elastic modulus and Poisson ratio are 7300kg/m^3, 140GPa and 0.26. While the material of screw shaft, motor shaft, etc. are steel, whose density, elastic modulus and Poisson ratio are 7800kg/m^3, 206GPa and 0.3. Moreover the main technical parameters are as follows: the torsional stiffness of coupling is $2.7\times10^4 N\cdot$ m/rad, the vertical stiffness and horizontal stiffness of linear guide are respectively 1.88×10^9N/m and 1.25×10^9N/m. The basic parameters of ball screw are as follows: the nominal diameter of lead screw, the diameter of ball and the contact pressure angle are 60mm, 9mm and 45°. The number of working cycles of balls is 8, and the effective length of screw is 105mm. Supposing that the contact type of ball-screw pair is point-contact and the screw and the nut are separately named as node S and node N, the connection between screw and nut could be simplified as the interaction between the two nodes belonging to different components. According to the product technical manual, the axial stiffness of screw-nut pair is 1.65×10^9 N/m, and its tangential stiffness 8.35×10^8 N/m, the torsional stiffness 9.4×10^3N$\cdot$m/rad, the bending stiffness 1.73×10^6N$\cdot$m/rad, and the coupling stiffness 3.94×10^6 N/rad. The rectangular coordinate system shown in Fig. 2 (a) is the global coordinate system whose X-axis is the axis direction of screw-shaft and Y-axis is vertical. In the process of multi-flexible-body dynamics modeling, the local coordinate systems can be established according to the modeling object, so as to facilitate model. For example, the cylindrical coordinate system, whose axial direction is the same with the X-axis of the global coordinate system, is used as the local coordinate system to describe the bearing model, so as to define conveniently the axial and radial stiffness of the bearing.

ABAQUS is used to construct the multiple-flexible-body dynamic model of the ball screw feed system. And through the grid checking tool in ABAQUS software, the failure rate of the grid quality of each structural part is 0, and the warning rate is less than 0.5%. So the optimized grid quality can be obtained and used. Remarkably, the reduced state space model is constructed by the constrained modes, which is namely the modes under the real boundary constraint state of ball screw feed system. The real boundary constraint state is that: the bottom of machine tool bed is constrained; the screw-nut mechanism exists in the ball screw feed system, that is to say, when the lead screw rotates, the worktable can move along the guide rail. Therefore, the simulation results show that the first mode is rigid body mode, i.e. zero, which accord with the actual situation and mode theory. The second mode begins to be a non-rigid body mode. Therefore, the first-order mode shapes given later in this paper are the first-order non-rigid mode shapes.

As explained previously in section 2.1, the structural vibration mainly depends on low-order modal-modes. And the number of low-order modal-modes for reduction can be determined according to the concerned frequency response bandwidth of excitation based on the determination rule mentioned in section 2.1.

Also the frequency response performance of servo control is affected by the vibration of mechanical transmission. The control signal only in the control bandwidth lower than natural frequency of mechanical structures can be transferred without delay and attenuation. Through FEA about the multi-flexible body dynamics model of this ball screw feed system, it can be obtained that: its first-order modal frequency is about 47 Hz (as shown in Fig. 2). This means that: the servo control signal of this ball screw feed system would begin to attenuate and delay after the lower frequency, which is lower than first-order natural frequency of mechanical structure.

Based on the above analysis, the motion response characteristics of this ball screw feed servo control system within the 300 Hz frequency bandwidth (including the motion response characteristics of mechanical transmission under the motor input torque within this bandwidth) are more focused in this paper. According to the low-order modal-modes selection rule mentioned in section 2.1, the modal-modes whose modal frequency less than 500 Hz are selected.

In this paper, FE software ABAQUS is used to construct the multiple-flexible-body dynamic model of the ball screw feed system, and also realizes its corresponding modal analysis. Through the finite element software and corresponding modal analysis, based on the FE multiple-flexible-body dynamic model of ball screw system, the coefficient matrix and mode shape matrix (In Eq. (7)) of structural dynamic model of ball screw feed system can be obtained with the help of FE software and the corresponding modal analysis. Then substituting these coefficient matrixes and mode shape matrixes into the Eq. (7), through MATLAB, the reduced state space model of ball screw feed system can be obtained. Also by solving its state space model equations through MATLAB,

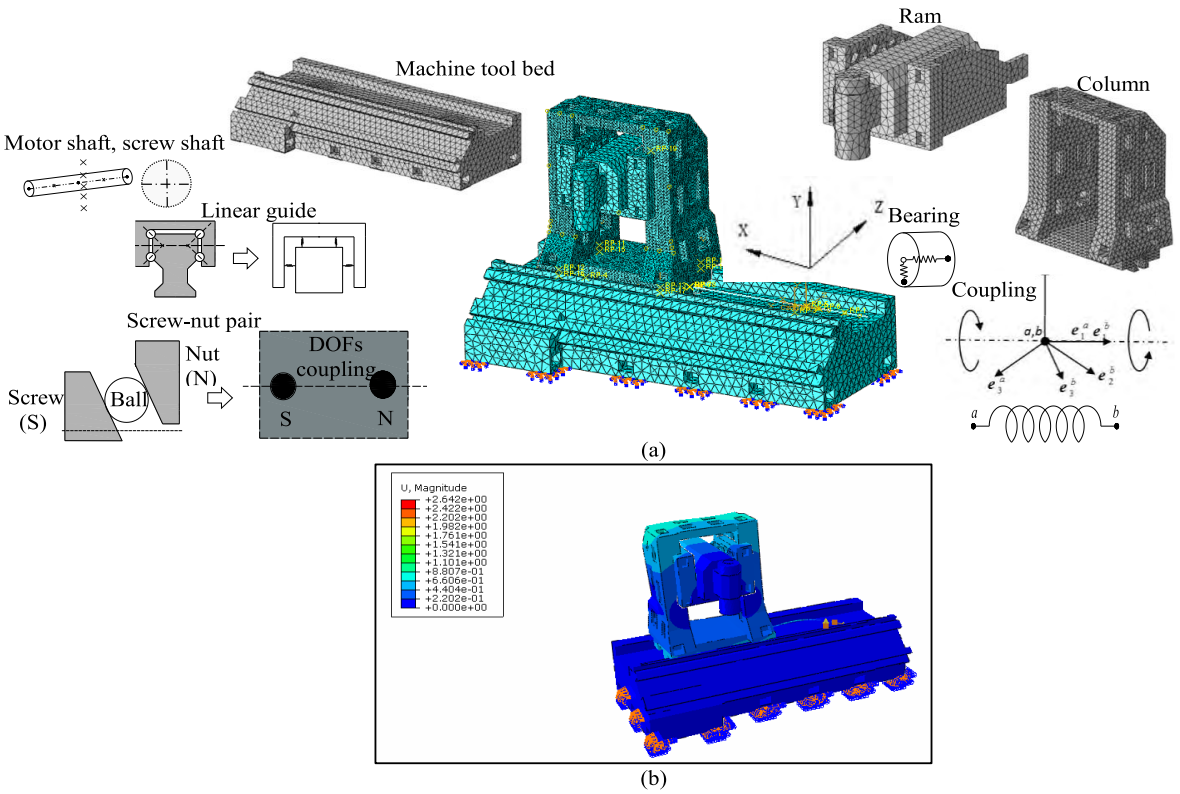

FIGURE 2. (a) Dynamic model of multi flexible body structure for ball screw feed system and (b) its modal shape (first order mode frequency 47.96Hz), mainly about the movement along the guided-rail (i.e. in X direction).

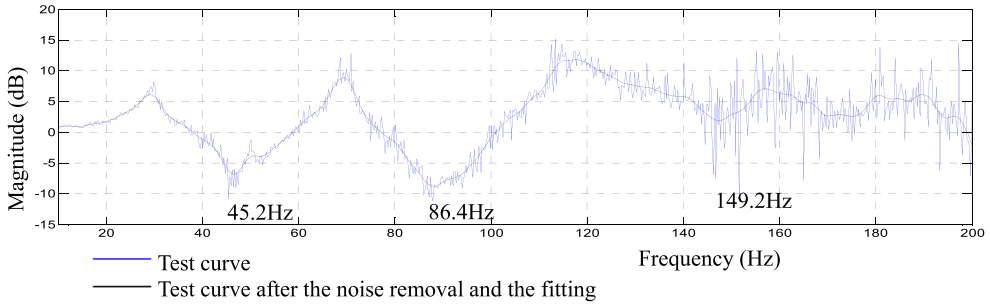

FIGURE 3. Mechanical frequency response curve from mechanical frequency test function integrated in Start-up tool.

the frequency response between actual speed and input torque of the feed system can be obtained.

C. EXPERIMENT VERIFICATION

The correctness of the multiple-flexible-body dynamic model and this reduced state space model of ball screw feed system is verified by experiments as follows: The machine tool studied in this paper adopts SIEMENS 840D SINUMERIK Numerical Control (NC) System [29], [30], which is the control system integrates all CNC system components into one operation panel, and are widely used in machine tool control. SIEMENS has successfully developed and integrated the response testing software and modules of servo control, which has been widely used in practice [26]–[28]. The test of dynamic response in this paper is based on the panel control unit (PCU50) and the integrated module tool (Start-up tool (IBN-Tool)) of operating interface software (HMI Advanced).

By the mechanical frequency test function integrated in Start-up tool (IBN-Tool) in this machine tool [29], [30], the test frequency response curve is obtained in Fig. 3 (the blue curve). By executing the noise removal and the fitting of curve, the mechanical frequency response curve is obtained in Fig. 3 (the black curve). As shown in Fig. 3, the nature frequencies by test are frequencies are respectively 45.2Hz, 86.4Hz and 149.2Hz. And the frequencies from FE simulation based on multiple-flexible-body dynamic model and also the mechanical frequency test through IBN-Tool are

TABLE 1. Compare of frequencies from experiment test and simulation based on multiple-flexible-body dynamic model.

	Natural frequency of system		
Experimental results	45.2Hz	86.4Hz	149.2Hz
Simulation results	47.96 Hz	90.74 Hz	142.16Hz
Relative error	5.7%	4.7%	4.9%

shown in Tab. 1. It can be seen that the frequencies from test (45.2Hz 86.4Hz and 149.2Hz) are consistent with the natural frequencies from simulation (47.96 Hz 90.74 Hz 142.16Hz). And the maximum relative error between the simulation and the experiments is 5.7%. Also the root mean square error (RMSE) is used to represent the comprehensive prediction accuracy of this multiple-flexible-body dynamic model. And RMSE can be obtained by calculation based on the Tab. 1, whose value is 5.03Hz. It represents the average deviation between the predicted frequency and the real frequency is 5.03Hz. All these show that the multi-flexible body modeling of the ball screw feed system is correct.

Notably, the mode-shapes of mode simulation results in Tab. 1 are about the relative rotation of the screw-shaft and the motor-shaft, and the movement of movable components such as the column under the screw-nut mechanism along the guide-rail. According to the mode synthesis method, the structural dynamic response in the physical coordinates can be superposed by the weighted mode shapes in the modal coordinates. And the superposition of the mode shapes with the same trend of motion caused by the excitation determines the response under this excitation. Therefore, through this mechanical frequency test function, the obvious resonance point (i.e. mechanical nature frequency) in the structural dynamic amplitude-frequency response curve (in Fig. 3) corresponds to the nature mode frequencies whose mode-shapes have the same motion trend generated by the input torque. That is to say, the frequencies obtained by this mechanical frequency test function correspond to the simulation modal frequencies whose mode-shapes are the relative rotation of the motor-shaft and screw-shaft, the movement of column alone guide-rail, as shown in Fig. 2 (b). Moreover, these modes are exactly that have the major impact on the motion response performance studied in this paper under the input torque.

In addition, by solving its state space model equations through MATLAB, the frequency response between actual speed and input torque of the feed system under the influence of modal characteristics can be obtained. Also the frequency response between speed and input torque can be got by experiment through IBN-Tool.

It is noteworthy that: the comparison and detailed analysis about this frequency response between actual speed and input torque from experiment and state space model are detailed in Figs. 13 and Tab. 6, which also include the frequency response between speed and input torque through hybrid dynamic modeling, so as to highlight the accuracy of ball screw feed system reduced state space model in solving the motion response compared to hybrid dynamic modeling without repetitive drawing. The frequency response between speed and input torque of the feed system under the influence of modal characteristics from simulation results are in good agreement with the experimental results, as explained in section in Figs. 13 and Tab. 6 in section 4.2 experiment results and result analysis, which verifies the correctness of this reduced state space model.

III. STEP-BY-STEP OPTIMIZATION METHOD OF BALL-SCREW FEED DRIVE SERVO PARAMETERS UNDER THE INFLUENCE OF STRUCTURE MODAL CHARACTERISTICS

On the basis of modal characteristics extraction of mechanical transmission based on state space (in Section 2), the step-by-step optimization method from the global to the local instead of traditional single-step optimization method is proposed in Section 3, so as to optimize the servo controller and the whole dynamic characteristic under the influence of structure flexibility and modal characteristics.

Firstly, the global initial optimal tuning of servo controller parameters under the influence of modal characteristics is carried out, through the analytic derivation calculation of servo controller based on the extraction of state space modal characteristics. And the global initial optimal tuning (In Section 3.1) includes:

Originally, the global initial optimization estimations of gain and delay time of speed loop are realized by synthesizing the complex ratio method with state space modal characteristics of ball screw feed system. (In Section 3.1.1)

Also originally, the constrain relational equation of gain of position loop considering modal characteristics and structure flexibility is derived, and also the global initial optimization estimation of gain of position loop is carried out by solving this constrain relation equation based on the recurrence method. (In Section 3.1.2)

Secondly, the integrated model of feed drive system is established. Additionally, by taking the calculated result above as the global optimization initial value, based on the optimization algorithm, the overall dynamic performance and servo controller of feed drive system under the influence of modal characteristics and structure flexibility of system are farther studied and optimized locally. (In Section 3.2)

What should be mentioned above all is that: the ball screw feed drive system of machine tool adopts generally the classical cascade controller, which includes the current loop, the speed loop and the position loop. The optimal control parameters of current loop can be obtained by the

motor manufacturer. Therefore, the optimization design of control parameters of speed loop and position loop are only conducted in this paper.

A. GLOBAL INITIAL OPTIMIZATION ESTIMATIONS OF SERVO CONTROL PARAMETERS BASED ON MODAL CHARACTERISTIC EXTRACTION OF FEED SYSTEM

1) OPTIMIZATION CALCULATION OF SPEED LOOP CONTROL PARAMETERS BY SYNTHESIZING COMPLEX RATIO METHOD WITH MODAL CHARACTERISTIC EXTRACTION

a: GLOBAL OPTIMIZATION CALCULATION METHOD OF SPEED LOOP CONTROL PARAMETERS

As mentioned above, the dynamic response of whole ball screw feed drive are influenced and restricted by the structure flexibility and modal characteristics greatly. Originally, the global initial optimization estimations of gain and delay time of speed loop are proposed by synthesizing the complex ratio method with state space modal characteristics of ball screw feed system, so as to consider the influence from the structure flexibility and modal characteristics fully.

Generally, the ball screw feed drive system widely adopts the classical cascade controller, which consists of the speed loop, the position loop, etc. In order to simplify the calculation, the current loop can be replaced by the P-T1 link with delay time T_{EI}^*, and the characteristic of this regulation loop can be regarded as the second order. So it can be obtained that $T_{EI}^* = 2T_{\sigma I} - 0.5T_{ATI}$, where T_{ATI} is the sampling time of current regulation loop, $T_{\sigma I}$ is sum of small delay time of current regulation loop. In general, $T_{\sigma I} = 2T_{ATI}$. So it can be obtained that: $T_{EI}^* = 3.5T_{ATI}$.

Furthermore, the speed regulation circuit is simplified and then modeled. The current regulation loop is replaced by its equivalent delay time, which is mentioned above. The sum of small delay time of speed regulation circuit includes the time delay of speed regulation circuit and the equivalent delay time of current regulation loop. Therefore, for the speed regulating circuit, its delay time $T_{\sigma n} = 1.5T_{ATn} + T_{EI}^*$, where $T_{\sigma n}$ is the sum of delay time of speed regulation circuit, which can be regarded as P-T1 link, and T_{ATn} is the sampling time of speed regulation loop. Based on the state space model of mechanical transmission module, the simplified model of speed regulation loop is obtained, as shown in Fig. 4, where K_{pn} is the gain of speed regulator, T_n is the integral time constant of speed regulator, ω_{des} represents the setting value of speed, and ω_{act} refers to the actual value of speed.

According to the complex ratio method [31], the frequency response of closed-loop speed control can all be transformed into the unified form of frequency characteristic equations presented in Eq. (8a). And if the specific value of two adjacent coefficient ratios can satisfy Eq. (8b), the favorable control characteristic can be obtained.

$$\begin{cases} F(jw) = \dfrac{b_0 + b_1 jw + \cdots b_{\mathrm{m}}(jw)^m}{a_0 + a_1 jw + \cdots a_{\mathrm{n}}(jw)^n} & \text{(a)} \\ a_i a_{i-2}/(a_{i-1})2 - 1/2 \le 0 & \text{(b)} \end{cases} \tag{8}$$

where a series of coefficient ratios can be constituted by the coefficients of denominator as follows: $a_n/a_{n-1}, a_{n-1}/a_{n-2}, a_{n-2}/a_{n-3} \ldots a_1/a_0$.

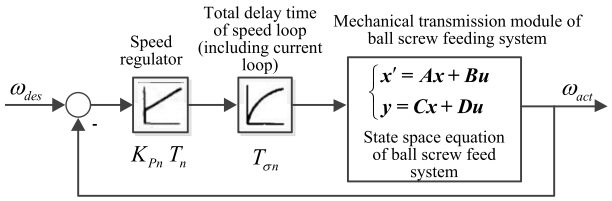

FIGURE 4. Simplified model of speed regulation circuit based on modal characteristic extraction by state space.

So through the speed regulation circuit based on modal characteristic extraction by state space as shown in Fig. 4, the frequency characteristic equation (Eq. (8a)), and series of coefficient ratios (Eq. (8b)) can be obtained. By solving this Eq. (8), the favorable speed control parameters considering the influence from the structure flexibility and modal characteristics fully can be reached.

b: OPTIMIZATION CALCULATION OF SPEED LOOP CONTROL PARAMETERS FOR THE BALL-SCREW FEED DRIVE STUDIED IN THIS PAPER

In this paper, parameters of feed drive system of NC machine tool studied is $T_{ATI} = T_{ATn} = 0.25$ms. So $T_{\sigma n} = 1.5T_{ATn} + 3.5T_{ATI} = 0.00125$s according to the formulas above. Base on the reduced state space model of ball screw feed system studied in Section 2, by combing with the simplified model of speed regulation loop in Fig. 4, all-order denominator coefficients in Eq. (8) for the ball screw feed drive studied in this paper can be got from the calculation by MATLAB:

$$\begin{cases} a_0 = 2.3e16K_{pn}, a_1 = 2.31e16K_{pn}T_n + 1.44e13K_{pn} \\ a_2 = 7.32e11K_{pn} + 3.75e15T_n + 1.42e13K_{pn}T_n \\ a_3 = 7.32e11K_{pn}T_n + 2.55e8K_{pn} + 6.99e12T_n \\ a_4 = 5.94e10T_n + 4.08e6K_{pn} + 2.55e8K_{pn}T_n \\ a_5 = 8.26e7T_n + 618.7K_{pn} + 4.08e6K_{pn}T_n \\ a_6 = 2.16e5T_n + 5.0K_{pn} + 618.7K_{pn}T_n \\ a_7 = 268.53T_n + 5.0K_{pn}T_n \end{cases} \tag{9}$$

By substituting Eq. (9) into Eq. (8)b, it can be obtained that: $a_i a_{i-2}/(a_{i-1})^2 - 0.5 \le 0, i = 2 - 7$. The optimization estimation value of the gain (K_{pn}) and the integral time (T_n) of speed loop can be obtained by solving this equation set: $a_i a_{i-2}/(a_{i-1})^2 - 0.5 = 0$.

By selecting the interval of K_{pn} and T_n as 0-30$Nm \cdot S/rad$ and 0-0.02s, through the discrete values of K_{pn} and T_n, the values about a_i and $a_i a_{i-2}/(a_{i-1})^2 - 0.5$ can be calculated and obtained. So six groups of surface graphics $(K_{pn}, T_n, (a_i a_{i-2}/(a_{i-1})^2 - 0.5))$ can be drawn out by MATLAB, which are shown in Fig. 5(a)-5(f).

As can be seen from these figures, the surface graphics of $(K_{pn}, T_n, (a_i a_{i-2}/(a_{i-1})^2 - 0.5))$ are similar with each other when $i = 2, 4, 6$; while the surface graphics of

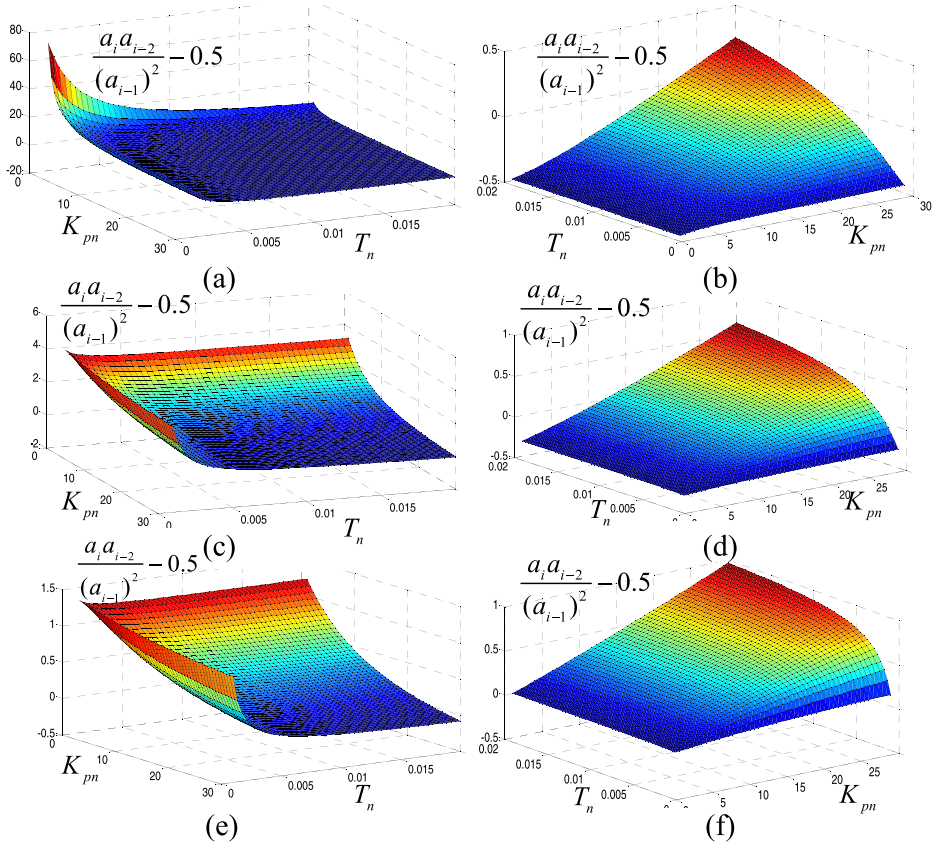

FIGURE 5. Surface plot about.$(K_{pn}, T_n, a_i(a_{i-1})^2 - 0.5)$.

$(K_{pn}, T_n, (a_i a_{i-2}/(a_{i-1})^2 - 0.5))$ are also similar when $i = 3, 5, 7$. In addition, it can be seen from Fig. 5(a), 5(c) and 5(e) that: in order to make the value of $(a_i a_{i-2}/(a_{i-1})^2 - 0.5)$ close to zero, the values of servo control parameter should be larger. While the situation is just the opposite in the Fig. 5(b), 5(d) and 5(f), the values of servo control parameter should be less so as to make the value of $(a_i a_{i-2}/(a_{i-1})^2 - 0.5)$ close to zero. By comprehensive analysis above, it can be seen that the selection of control parameters (K_{pn} and T_n) is contradictive.

Because of the number of parameters (K_{pn} and T_n) to be solved is less than the number of equations $(a_i a_{i-2}/(a_{i-1})^2 - 0.5 = 0, i = 2 - 7)$, these equations are indeterminate. By solving these indeterminate equations (9) $(a_i a_{i-2}/(a_{i-1})^2 - 0.5 = 0, i = 2 - 7)$ with the help of the graphics in Fig. 5, $K_{pn} = 21\text{Nm} \cdot \text{s/rad}$ and $T_n = 10\text{ms}$ are obtained finally.

2) OPTIMIZATION CALCULATION OF POSITION LOOP GAIN BASED ON THE DERIVATION OF ITS CONSTRAIN RELATION EQUATION

In this section, originally, the constrain relation equation of position loop gain considering modal characteristics and structure flexibility is derived firstly. And then the global initial optimization estimation of position loop gain is carried out by solving this constrain relation equation based on the recurrence method.

a: CONSTRAIN EQUATION DERIVATION OF POSITION LOOP GAIN CONSIDERING MODAL CHARACTERISTICS AND STRUCTURE FLEXIBILITY

The simplified model of position regulation loop based on modal characteristic extraction from state space matrix is constructed firstly, so as to derivate and optimize the position loop gain under the influence of structural flexibility and modal characteristics.

The position regulating circuit comprises the speed regulating circuit, also the link with pure time delay, and the sample-and-hold link of position control loop, etc. In order to simplify the analysis and solve the problem easily, the magnitude response characteristics of the link with pure time delay and the sample-and-hold link can be omitted. Because the amplitude frequency response of the link with pure time delay is characterized by constant 1, it has no effect on the amplitude of frequency response characteristic of overall system and it can be omitted. In order to simplify the analysis and solution of the amplitude response characteristics of the position loop, the sampling and holding link is omitted. So the simplified model of position regulation loop based on the modal characteristic extraction from state space matrix can be obtained finally, which is shown in Fig. 6, where T_{Gn} is the delay time

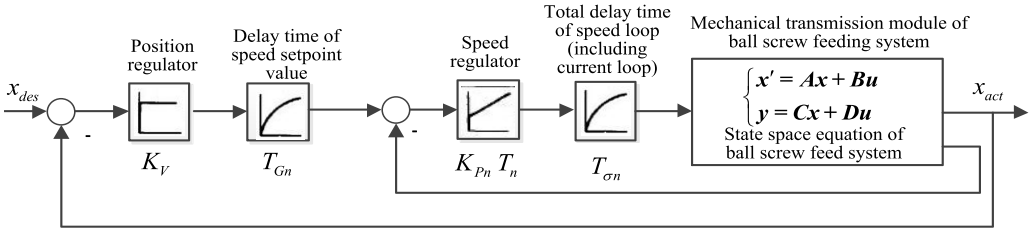

FIGURE 6. Simplified model of position regulation loop based on the modal characteristic extraction from state space matrix.

of speed set-point value, K_V is the position loop gain, x_{act} and x_{des} are the actual value and set value of the position.

The magnitude response curve of speed regulation loop has the peaking value at the position of natural frequency of mechanical transmission. It can be known by analysis that this peaking value is affected by the mechanical transmission and the speed regulation loop together, which is related to the servo control parameters, the structural vibration and modal characteristics. Through the optimization calculation process of speed regulation loop in Section 3.1.1, this peaking value can be obtained easily, which is defined as H_V.

The selection principle of gain (K_V) of position regulation loop is to reduce the response time of system as far as possible, namely that K_V should be as large as possible under the condition that the position loop is not overshoot. The overall open-loop amplitude characteristic can be obtained by multiplying the absolute value of frequency response characteristics of each link in Fig. 6. The absolute value of amplitude frequency response characteristic of position open loop at the natural frequency can be expressed as:

$$|F_s| = K_V \frac{1}{\sqrt{1 + w^2 T_{Gn}^2}} \frac{1}{w} H_V \tag{10}$$

where w is natural cycle frequency of system.

In order to ensure that the closed loop of position is not overshoot (not more than 0dB), the frequency response characteristic of open loop of position requires the enough magnitude margin. The magnitude margin of open loop of position can be defined as XdB, namely $|F_s| \leq 10^{\frac{-X}{20}}$. By assuming that $10^{\frac{-X}{20}}$ equals Y, so $|F_s| \leq Y$. By substituting $|F_s| \leq Y$ into Eq. (10), it can be obtained as follows:

$$K_V \leq Y \frac{1}{H_V} w \sqrt{1 + w^2 T_{Gn}^2} \tag{11}$$

In addition, the relation exists between the sum of small delay time of position loop and control parameter of position loop as follows [31]:

$$K_V \leq 1/(2T_{\sigma x}) \tag{12}$$

where, $T_{\sigma x}$ is the sum of small delay time of position loop. $T_{\sigma x}$ includes the equivalent delay time of speed regulating circuit (T_{En}^*), the delay time of speed set-point value (T_{Gn}) and the pure delay of position regulation loop (T_{tx}), namely that

$$T_{\sigma x} = T_{En}^* + T_{Gn} + T_{tx} \tag{13}$$

In fact, it can be seen from that Eq. (11) and Eq. (12) all restrict K_V at the same time and also T_{Gn} is included by $T_{\sigma x}$. Also it shows by analysis that Eq. (12) is the decreasing function of $T_{Gn}(T_{\sigma x})$, Eq. (11) is the increasing function of T_{Gn}. So the optimal conditions that the maximum K_V satisfies Eq. (11) and Eq. (12) at the same time is that

$$Y \frac{1}{H_V} w \sqrt{1 + w^2 T_{Gn}^2} = \frac{1}{2T_{\sigma x}} \tag{14}$$

The above formulation can be converted into:

$$2Y \frac{1}{H_V} \sqrt{1 + w^2 T_{Gn}^2} = \frac{1}{wT_{\sigma x}} \tag{15}$$

After the above formulation is divided by $wT_{\sigma x}$, it can be obtained that:

$$2Y \frac{1}{H_V} \sqrt{\frac{1}{(wT_{\sigma x})^2} + \frac{T_{Gn}^2}{T_{\sigma n}^2}} = \frac{1}{(wT_{\sigma x})^2} \tag{16}$$

By defining that $\frac{1}{(wT_{\sigma x})^2} = x_1, 2Y\frac{1}{H_V} = a$ and $\frac{T_{Gn}^2}{T_{\sigma n}^2} = b$, Eq. (16) can be rewritten as:

$$a\sqrt{x_1 + b} = x_1 \tag{17}$$

By solution, it can be obtained that: $x_1 = \frac{a^2 \pm a\sqrt{a^2+4b}}{2}$ (because $b > 0$ and $x_1 > 0$, $\frac{a^2 - a\sqrt{a^2+4b}}{2}$ is taken out). So $x_1 = \frac{a^2 + a\sqrt{a^2+4b}}{2}$, namely that:

$$\frac{1}{(wT_{\sigma x})^2} = \frac{2Y^2}{H_V^2} + \frac{2Y}{H_V} \sqrt{\frac{Y^2}{H_V^2} + \frac{T_{Gn}^2}{T_{\sigma x}^2}} \tag{18}$$

By multiplying Eq. (11) with Eq. (12) ($K_V \leq 1/2T_{\sigma x}$), the following formulation can be got:

$$K_V^2 \leq \frac{Y}{2} \frac{1}{T_{\sigma x}} \frac{1}{H_V} w \sqrt{1 + w^2 T_{Gn}^2} \tag{19}$$

From Eq. (19), Eq. (20) can be derived as:

$$\frac{K_V^2}{w^2} \leq \frac{Y}{2} \frac{1}{T_{\sigma x}} \frac{1}{H_V} \sqrt{\frac{1}{w^2} + T_{Gn}^2} = \frac{Y}{2} \frac{1}{H_V} \sqrt{\frac{1}{w^2 T_{\sigma x}^2} + \frac{T_{Gn}^2}{T_{\sigma x}^2}} \tag{20}$$

Finally, by substituting Eq. (18) into Eq. (20), the constrain relation equation of gain of position loop can be obtained as follows:

$$\frac{K_V^2}{w^2} \le \frac{Y}{2}\frac{1}{H_V}\sqrt{(\frac{2Y^2}{H_V^2}+\frac{2Y}{H_V}\sqrt{\frac{Y^2}{H_V^2}+\frac{T_{Gn}^2}{T_{\sigma x}^2}})+\frac{T_{Gn}^2}{T_{\sigma x}^2}} \quad (21)$$

b: GLOBAL OPTIMIZATION CALCULATION OF POSITION LOOP GAIN BASED ON ITS CONSTRAIN RELATION EQUATION

It can be seen from the constrain relation equation of gain of position loop in Eq. (21) that: when Y is determined (namely the magnitude margin of open loop of position (X) is determined), the value of K_V depends on: the ratio ($T_{Gn}/T_{\sigma x}$), w (natural cycle frequency of feed drive system), H_V (peaking value of speed regulation loop at the natural frequency, which is affected greatly by the structural vibration and modal characteristics of the mechanism).

So this constrain relation equation of gain of position loop considering modal characteristics and structure flexibility can be solved, so as to get the global initial optimization estimation of gain of position loop. The recurrence method combined by graphical method is introduced here to solve this constrain relational expression as follows:

Step 1: the magnitude margin of open loop of position (X) is determined as required firstly. So $Y(Y = 10^{-X})$ is determined also. Then, according to constrain relational expression in Eq. (21), the relation curve graphic between K_V/w and $T_{Gn}/T_{\sigma x}$ with different H_V can be drawn easily.

Step 2: the value of T_{Gn} is set by attempts (starting from 0 and in ascending order). Then the value of $T_{\sigma x}$ can be calculated according to Eq. (13). And also the value of $T_{Gn}/T_{\sigma x}$ can be obtained.

Step 3: according to the relation curve graphic (the relation curve graphic between K_V/w and $T_{Gn}/T_{\sigma x}$ with different H_V) in Step1, the value of K_V/w corresponding to different H_V and $T_{Gn}/T_{\sigma x}$ in Step2 is obtained easily. Then the value of K_V can be also obtained based on the value of K_V/w and w.

Step 4: the value of K_V obtained in Step3 is judged by constraint condition (Eq. (12) $K_V \le 1/2T_{\sigma x}$). If the value of K_V obtained in Step3 can satisfy the constraint condition ($K_V \le 1/2T_{\sigma x}$), Step2 is repeated with bigger value of T_{Gn}. If the value of K_V obtained in Step3 can't satisfy the constraint condition ($K_V \le 1/2T_{\sigma x}$), the recursive calculation can't be continued. And the value of K_V in previous recursive calculation is chosen as the final value.

c: OPTIMIZATION CALCULATION OF POSITION LOOP GAIN FOR THE BALL-SCREW FEED DRIVE STUDIED IN THIS PAPER

For the ball screw feed drive system studied in this paper, the global initial optimization estimation of K_V is carried out by the above constrain relation equation of position loop gain and its solution as follows:

In this paper, the open loop magnitude margin is defined as 8dB ($X = 8$ and $Y = 0.4$). Also, according to the speed regulation loop model based on modal characteristic extraction from state space matrix in Section 3.1.1, the peaking point of magnitude response of closed speed loop can be solved, which is shown in Fig. 7. Due to the influence of closed loop servo control, these peaking points deviate from the original natural frequencies of mechanical transmission, which are located in 52.64Hz, 99.33Hz and 160.2Hz. And the corresponding peaking value (H_V) are −0.5081dB (0.9432), −0.6956dB (0.9230) and 1.219dB (1.1507). Besides, under the comprehensive influence of mechanical system and servo control system, the speed regulation circuit based on modal characteristic extraction has also the peaking point in 18.02Hz (it is mainly determined by the first-order natural frequency of mechanical transmission and also the frequency response characteristics of servo control system), whose peaking value is 3.52dB(1.4997) with overshoot. Then, according to constrain relation equation in Eq. (21), the relation curve between K_V/w and $T_{Gn}/T_{\sigma x}$ with different H_V can be drawn as in Fig. 8.

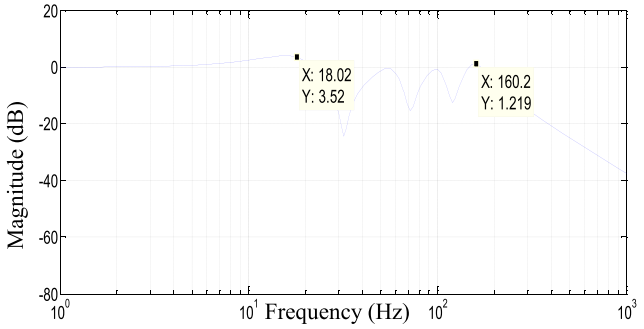

FIGURE 7. Peaking point of magnitude response of speed closed loop.

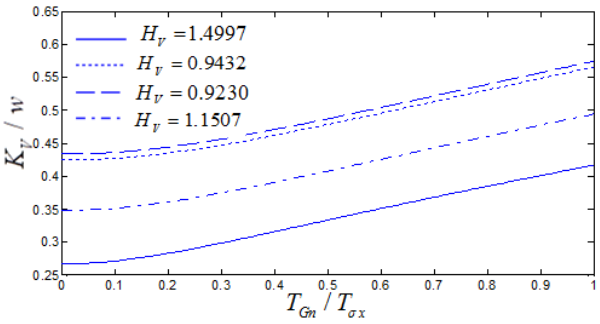

FIGURE 8. Relation curve graphic between K_V/w and $T_{Gn}/T_{\sigma x}$ with different H_V K_V/w.

As can be seen from Fig. 8, the curves are intensive on the top and sparse at the bottom. And with the increase of the peaking value (H_V), the trend of value of K_V is to decrease. That is to say, in order to maintain the stability of system (which is not overshoot), the allowable K_V decreases with the increase of H_V, which is consistent with the tuning experience of three loops of control system.

Because of the possibility of position overshoot in the four peaking points, it is necessary to carry on the calculation in all these four peaking points according to the above constrain relational expression (Eq. (21)) and its recurrence solution.

For the ball screw feed system studied in this paper, the parameters (T_{tx} and T^*_{En}) in Eq. (13) are respectively that: $T_{tx} = 1.5T_{ATx}$ and $T^*_{En} = 2T_{\sigma n} - 0.5T_{ATn}$, which are same with the calculation of the pure delay time of speed loop and equivalent delay time of current loop, as mentioned in Section 3.1.1. And T_{ATx} is the sampling time of position regulation loop. The speed regulation loop parameters ($T_{\sigma n}$ and T_{ATn}) has been obtained by relative calculation in Section 3.1.1, and $T_{\sigma n} = 0.00125$s, $T_{ATn} = 0.25$ms. The sampling time of position regulation loop T_{ATx} equals 0.004s for the ball screw feed system studied in this paper. Therefore it can be obtained that $T_{tx} = 6$ms and $T^*_{En} = 2.375$ms.

TABLE 2. The allowable values of K_V in first recurrence.

$w/2\pi$	18.02	52.64	99.33	160.2
K_V / w	0.2667	0.4241	0.4334	0.3476
$K_V(\mathrm{s}^{-1})$	30.20	140.27	270.49	349.88

If $T_{Gn} = 0$, by Eq. (13), it can be got that $T_{\sigma x} = 0.008375$s. Also it can be obtained from Fig. 8 that the corresponding value of K_V/w are shown in Tab. 2. Moreover the allowable value of K_V are derived by solution which are also shown in Tab. 2. It can be seen from Tab. 2 that K_V determined by the peaking point and its value is $30.20\mathrm{s}^{-1}$. And also the value of K_V determined by Eq. (12) ($K_V \leq 1/2T_{\sigma x}$) is that: $K_V \leq 1/(2T_{\sigma x}) = 59.7015\mathrm{s}^{-1}$, which is larger than the former K_V determined by the peaking point and its value. So the recursive calculation can be continued.

TABLE 3. The allowable values of K_V in second recurrence.

$w/2\pi$	18.02	52.64	99.33	160.2
K_V / w	0.3002	0.4487	0.4576	0.3760
$K_V(\mathrm{s}^{-1})$	33.97	148.33	285.45	378.28

Similarly, if $T_{Gn} = 4$ms, it can be got that $T_{\sigma x} = 0.012375$s by Eq. (13), and also $T_{Gn}/T_{\sigma x} = 0.3232$. So the corresponding K_V/w obtained from Fig. 8 are shown in Tab. 3. Moreover the allowable value of K_V are derived by solution which are also shown in Tab. 3. From Tab. 3, it can be known that K_V determined by the peaking point and its value is $33.97\mathrm{s}^{-1}$. And also the value of K_V determined by Eq. (12) ($K_V \leq 1/2T_{\sigma x}$) is that: $K_V \leq 1/(2T_{\sigma x}) = 40.40\mathrm{s}^{-1}$, which is larger than the former K_V determined by the peaking point and its value. These show that the recursive calculation can be continued also.

TABLE 4. The allowable values of K_V in third recurrence.

$w/2\pi$	18.02	52.64	99.33	160.2
K_V / w	0.3299	0.4735	0.4821	0.4025
$K_V(\mathrm{s}^{-1})$	37.33	156.53	300.73	404.94

The further recursive calculation is conducted. Similarly, if $T_{Gn} = 8$ms, also it can be got that $T_{Gn}/T_{\sigma x} = 0.4885$ finally. Moreover the allowable value of K_V are derived by calculation which are also shown in Tab. 4. In this table, it can be seen that K_V determined by the peaking point and its value is $37.33\mathrm{s}^{-1}$. Besides, the value of K_V determined by Eq. (12) ($K_V \leq 1/2T_{\sigma x}$) is that: $K_V \leq 1/(2T_{\sigma x}) = 30.53\mathrm{s}^{-1}$. It is less than the former K_V determined by the peaking point and its value, which doesn't satisfy the condition. So the recursive calculation can't be continued. Therefore the global initial optimization estimation of K_V by solving constrain relational express in Eq. (21) through recurrence method is $33.97\mathrm{s}^{-1}$, which can be approximated as $34\mathrm{s}^{-1}$.

From the above graphical-solution recursive procedure, it can be known that the first order frequency has the greater influence on the optimal design of position loop gain (K_V) in the all nature frequencies of system. That is to say, in this paper, the peaking point of magnitude response (located in 18.02Hz), mainly determined by the first-order natural frequency of mechanical transmission and also the frequency response characteristics of servo control system together, plays the major limitation effect on K_V.

However, the situation is different in the above optimization of the control parameter of speed loop. From the optimization calculation process of speed-loop control parameters in Section 3.1.1, the first few nature frequencies all have the great influence on the optimization design of control parameters (K_{pn} and T_n) of speed loop, which results that the influence of first few natural frequency should be considered all in the optimization selection for K_{pn} and T_n.

B. FURTHER LOCAL OPTIMIZATION OF WHOLE DYNAMIC PERFORMANCE AND SERVO PARAMETERS OF BALL SCREW FEED SYSTEM

In Section 3.1, through the analytic derivation calculation of servo controller based on the extraction of state space modal characteristics, the global initial optimal tuning of servo controller parameters under the influence of modal characteristics is carried out.

In this section, the local optimization after global initial optimal tuning is conducted. The overall dynamic performance and servo controller the under the influence of modal characteristics of system are further optimized, by taking the global initial optimal tuning of servo controller parameters above as the initial value.

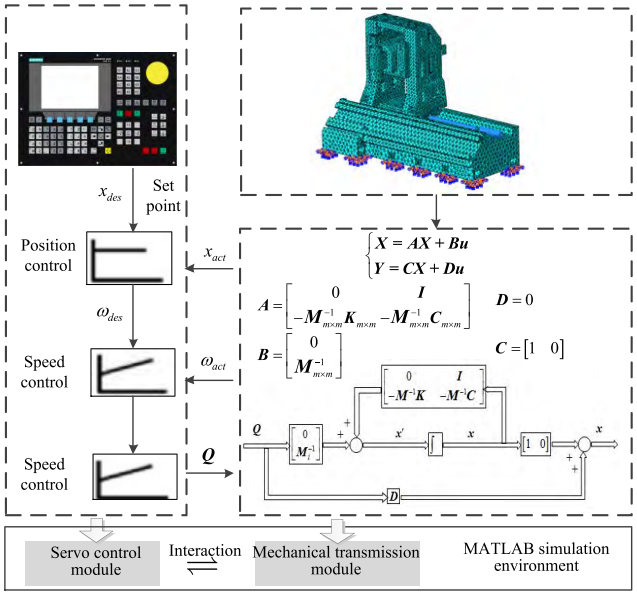

FIGURE 9. schematic diagram for integrated modeling of ball screw feed drive system.

Above all, by the same simulation environment, integrated modeling of ball screw feed drive system is established. Based on the digital module simulation method, the ball screw feed drive system can be divided into the mechanical transmission module and the servo control module. The mechanical transmission module of ball screw feeding system expressed by reduced state space matrix has been constructed and modeled by MATLAB in Section 2. Also the servo control module could be constructed by MATLAB. So the schematic diagram for integrated modeling of ball screw feed drive system is shown in Fig. 9. The main technical parameters of servo control system are that: the gain of current loop $K_i = 12.157\text{V/A}$, the integration time of current loop $T_i = 2\text{ms}$, the inductance coefficient $L_a = 3.1\text{mH}$, the resistance coefficient $R_a = 0.075\Omega$, the back-emf coefficient $K_e = 1.67\text{V/(rad/s)}$, and the torque coefficient $K_T = 2.72\text{N}\cdot\text{m/A}$.

In order to evaluate the dynamic performance of whole feed drive system, the following response characteristics can be used for the measure: the overshoot, integral of error between the ideal and actual displacement curve, the settling time, the rising time, etc. According to the different optimization design problems, the selection of target evaluation function is also not same; the common used objective functions are Square Error Integral (ISE), Absolute Error Integral (IAE), Time Multiplication Square Error Integral (ITSE) [37], and so on, which are the system response performance index expressed by the integral function of the deviation between ideal output and actual output of servo system.

If the above response characteristics are defined as the system performance index (*SPI*), based the principle of quadratic-type evaluation index, the objective evaluation function (*OEF*) of dynamic characteristics of whole feed drive system can be defined as:

$$OEF = \left(\prod_{i=1}^{n} [f_i(SPI_i)^{w_i}]\right)^{1/\sum_{i=1}^{n} w_i} \tag{22}$$

where, n represents the number of *SPI*, w_i refers to the weight of the single performance index in the overall evaluation function. Comprehensively, ITSE standard is chosen to evaluate the response speed of ball screw feed system, and also the function in Eq. (23) [32] is selected to assess the system's overshoot and transient oscillation:

$$SPI_2 = \int [f_o(t)e_o + f_s(t)e_s]dt \tag{23}$$

$$\text{with} \begin{cases} e_o = |x_{des} - x_{act}| & for\ (x_{des} - x_{act} < 0) \\ e_s = x_{des} - x_{act} & for\ (x_{des} - x_{act} > 0) \end{cases} \tag{24}$$

where e_s represents response error due to transient oscillation, e_o represents response error due to overshooting, f_o and f_s are coefficient functions. The weights of overshoot and transient oscillation can be controlled by selecting the value of f_o and f_s. In the position loop, the overshoot phenomenon should be strictly avoided. Therefore, the larger f_o can be chosen. In the optimization process in this paper, $w_1 = w_2 = 1, f_1 = 100, f_2 = 1, f_o(t) = 100$ and $f_s(t) = 25t^2$ In this section, the gain (K_V) of position loop, the gain (K_{pn}) and the integration time (T_n) of velocity loop are chosen as the optimization variables.

By taking the global analytic derivation of servo controller in Section 3.1 as the initial values, also by defining this initial value as the center of the optimization interval based on optimization algorithm, by choosing Eq. (22) as the optimization objective function to comprehensively evaluate response speed and overshoot and also transient oscillation, the further optimization of the overall dynamic performance and servo control parameters under the influence of modal characteristics are carried out. Finally, the optimal parameters of servo controller under the influence of the modal characteristics are obtained as follows $K_V = 38\text{s}^{-1}$, $K_{pn} = 24\text{Nm}\cdot\text{s/rad}$ and $T_n = 19\text{ms}$.

In order to compare with experiment result easily at the same time, the dynamic characteristics of this ball screw feed drive system before and after optimization are presented in **Section 4**, and the step response curves before and after optimization are all shown in Fig. 14, which aren't repeated here.

IV. EXPERIMENT TEST AND RESULT ANALYSIS

A. PRINCIPLE AND SCHEME OF THE EXPERIMENT

In this paper, based on the built-in sensor of the machine tool, the running state information of feed drive system is obtained, and also its dynamic performance is tested. In other words, the ontology information obtained from the encoder, servo motor current (torque) sensor and other sensors, which are integrated and installed in the feed system of the machine, are used here to test the operation response and dynamic performance of feed drive system. The signal of built-in sensor

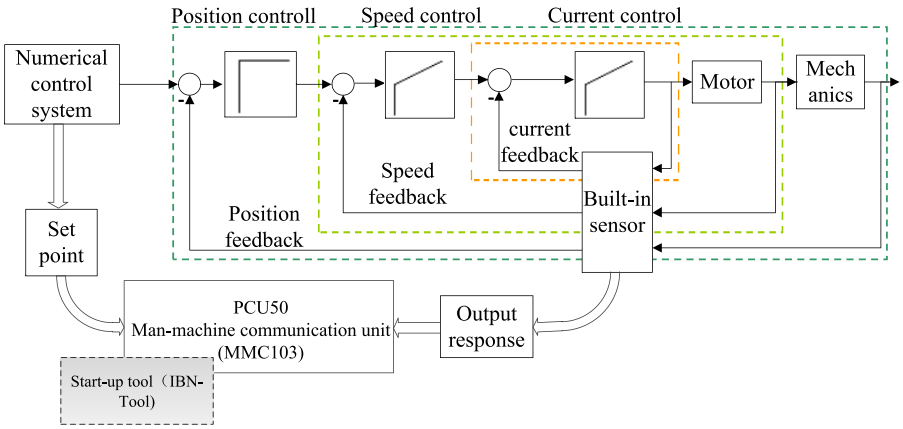

FIGURE 10. Experiment scheme of dynamic characteristics of ball screw feed drive system based on built-in sensor.

TABLE 5. Hardware and software for dynamic performance test of ball screw feed drive system.

Hardware	Notes
Man-machine communication unit MMC103 (PCU50)	Integrated in the SIEMENS SIMUMERIK 840D CNC system, see Fig. 12 (a)
Numerical control and driving unit NCU573.2	
Servo drive SIEMENS 611D	
Servo motor 1FT6136	None
Built-in sensors, such as electrical vortex sensor, encoder, etc.	
Software	**Notes**
Operating system Windows NT	None
Operating interface software Start-up tool（IBN-Tool）	Integrated and installed in operating interface software (HMI Advanced)

is the feedback of servo control system of machine tool. And it is the direct reflection of dynamic response characteristics of feed drive system, which includes input and output signals during the operation of feed drive system. So the information from built-in sensors integrated and installed in the feed system of the machine is ideal for dynamic performance testing of the feed system. Also, the dynamic performance test of feed drive system based on built-in sensor does not require external sensors, and only needs the sensors of machine tool itself, which avoids the limitations such as equipment cost, installation location and so on.

The dynamic performance test of machine tool feed drive system based on built-in sensor technology has been adopted by many scholars in their studies [33]–[35]. Also, based on the built-in sensor detection technology, SIEMENS has developed the related debugging tool and test function of feed drive dynamic performance, which is integrated in its CNC system. The test of dynamic characteristics of ball screw feed drive system in this paper is based on the debugging tool and test function integrated in SIEMENS 840D SINUMERIK NC system [29], [30]: the panel control unit (PCU50), and also the integrated module tool (Start-up tool (IBN-Tool)) of operating interface software (HMI Advanced). The scheme for dynamic characteristics test of ball screw feed drive system based on built-in sensor is shown in Fig. 10. The hardware and software for dynamic performance test of ball screw feed drive system are shown in Tab. 5.Human-computer interaction interface, Servo driver, PCU50, and the test in field are shown in Fig. 11.

B. EXPERIMENT RESULTS AND RESULT ANALYSIS

In these experiments, the position of nut is in the middle of the screw, which is the same with the position in the simulation model. The frequency response curve between the actual speed and the input torque based on the state space model of ball screw feed system is shown in Fig. 12. And the corresponding comparison between this experimental test and simulation is shown in Tab. 6.

By comprehensive analysis of Fig. 12 and Tab. 6, it can be seen that: the poles of magnitude response are consistent with the inherent frequencies of feed system basically, and the first and second order natural frequency are 47.96Hz and 90.74Hz by simulation, which are closed to the measure experiment (45.44Hz and 85.94Hz). The error of first order frequency between measurement and simulation is 5.54%. At the natural frequency of magnitude response curve, the differences between the measured results and the simulation are all about 3dB. The frequency response between speed and input torque of the feed system under the influence of modal characteristics from simulation

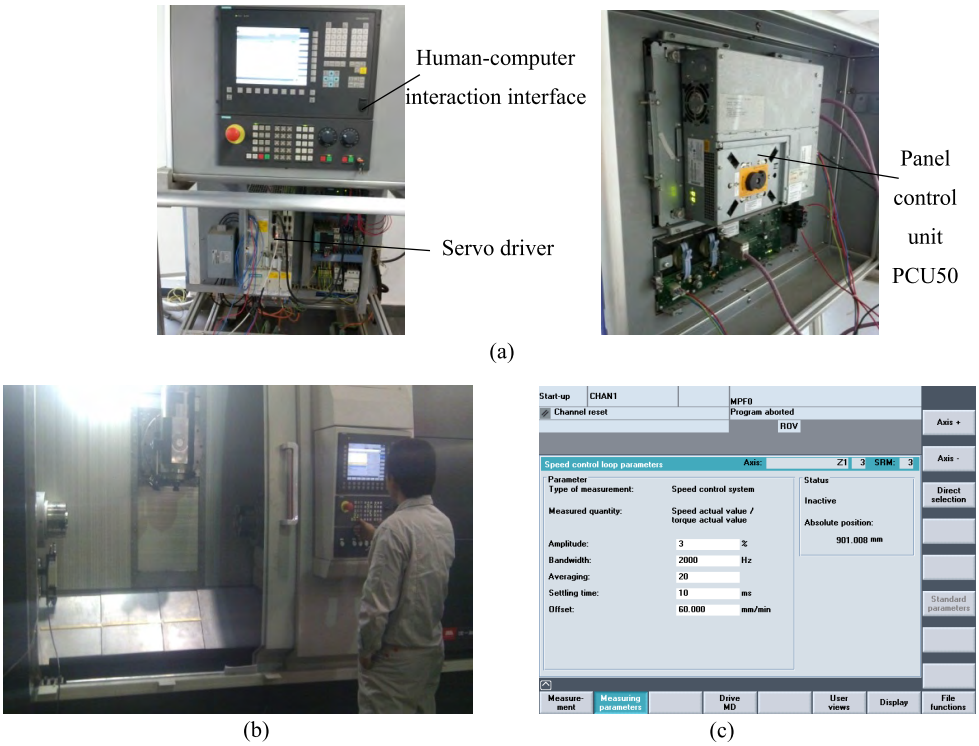

FIGURE 11. (a) Human-computer interaction interface, Servo driver and PCU50; (b) test in field; (c) test parameters setting.

TABLE 6. The comparison of frequency response curve between speed and input torque from experimental test and simulations.

	Coordinates of poles (at mechanical natural frequencies)		
Measurement	(45.44Hz,32.83dB)	(85.94Hz,28.93dB)	(130.9Hz,28.1dB)
Simulation from reduce state space	(47.96Hz,35.16dB)	(90.74Hz,32.17dB)	(142.16Hz,31.36dB)
Simulation from hybrid dynamic model	(66.83Hz,30.81dB)	(122.5Hz,28.52 dB)	(194.9Hz,27.56dB)

results are in good agreement with the experimental results.

In addition, the simulation result from the model as shown in Fig. 12, which is constructed through hybrid modeling method [24] by simplifying the moveable structure components of ball screw feed system with lumped mass is also compared. The frequency response curve between speed and input torque based on hybrid dynamic model deviates greatly from the experimental curve (as shown in Fig. 12). And its first natural frequency is predicted as 66Hz by simulation, which deviates greatly from the measure experiment (45.44Hz), as shown in Tab. 6. By comprehensive analysis of Fig. 12 and Tab. 6, it also can be seen that: the state space modeling of ball screw feed system based on multi-flexible body dynamics model can more accurately predict the motion response performance under the influence of structural flexibility and modal characteristics.

All above show the accuracy and validity of extracting modal characteristics of ball screw feed system based on the reduced state space, which can accurately solve the motion response performance under the influence of modal characteristics.

According to the above comparative analysis, it can be boldly inferred that: if the lumped mass method simplifying all structure component into lumped mass is used to model the ball screw feed system, the prediction accuracy of its motion response would be worse, which has been explained in the introduction of the relevant research about lumped mass method and hybrid model method.

Also the frequency response curve between the setting speed and the actual speed can be obtained by the integration model of ball screw feed drive system, and the corresponding test curve is obtained by experiment, which are all shown in Fig. 13. It can be seen from this figure that: due to the influence of the closed loop servo control, the pole position of magnitude response curve deviates slightly from the inherent frequency of mechanical transmission system. And the first pole positions are respectively (50.45Hz, −1.78dB) and (47.12 Hz, −4.46dB) in simulation and experiment. Also this simulation results are in good accordance with the

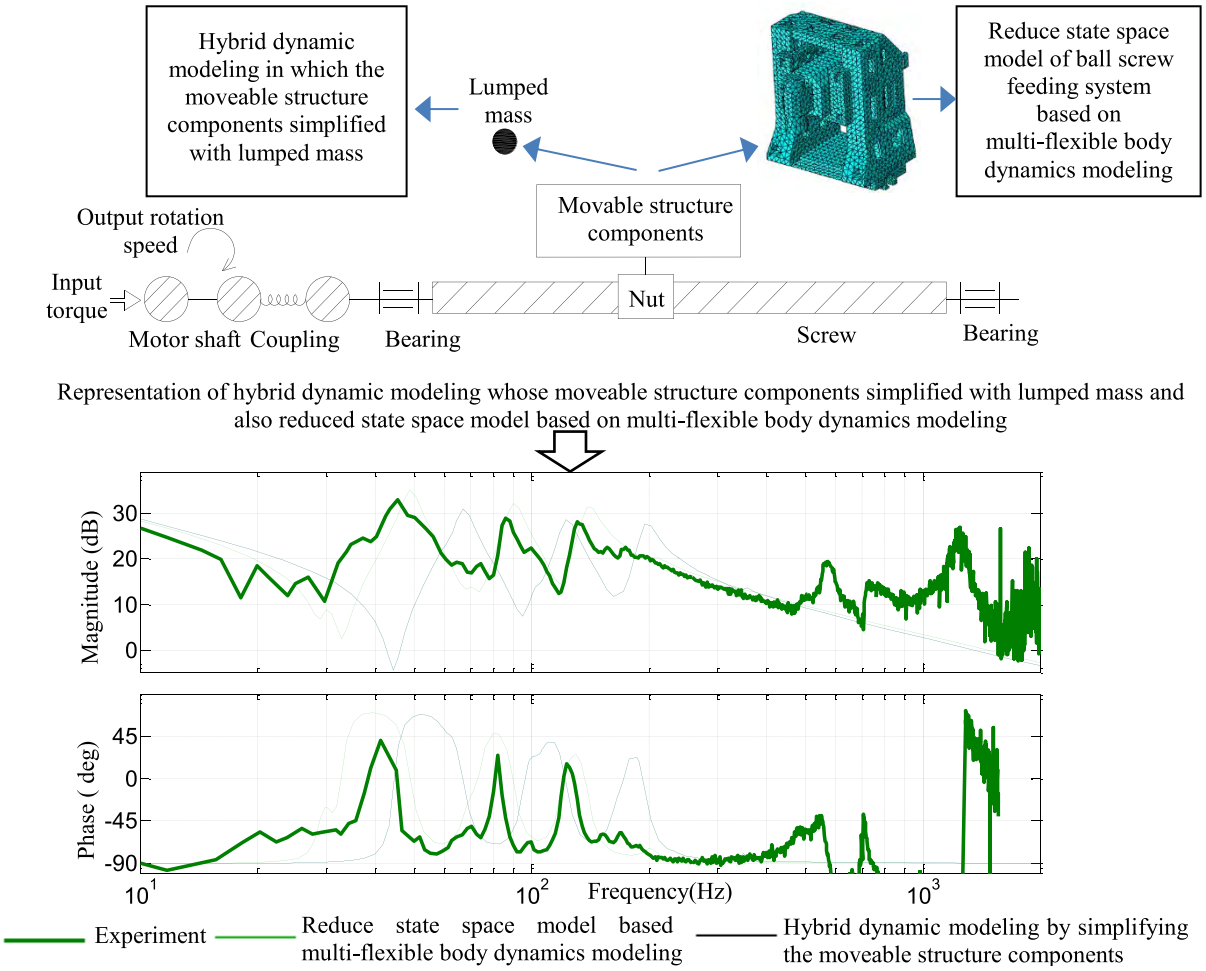

FIGURE 12. Frequency response curve between speed and input torque of the feed system.

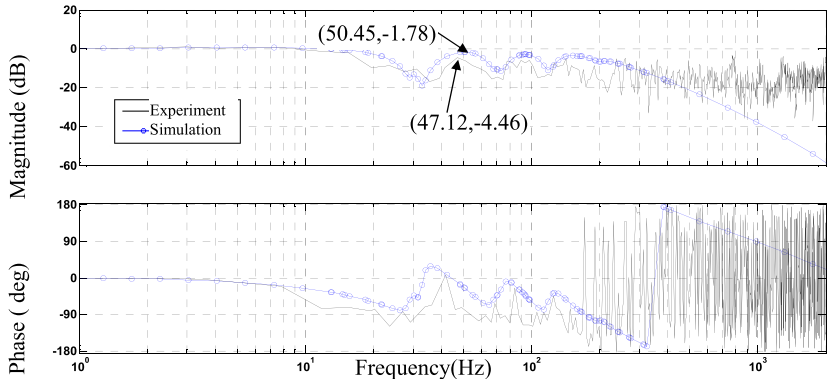

FIGURE 13. Frequency response curve between the setting speed and the actual speed.

experimental results on the whole, which shows the correctness of this integration model of ball screw feed drive system.

The comparison of the optimization results of step response of position loop obtained by three methods are shown in Fig. 14(a). Thereinto, Case1: the response result through the self-tuning method based on the approximate model analysis; Case 2: the optimization response result through self-tuning method based on optimization rules; Case 3: the response result through the proposed method. The rise times of Case 1, 2 and 3 are respectively 0.088s, 0.079s and 0.038s. Also it can be from the step response curve in Fig. 14(a), the response result through the proposed method

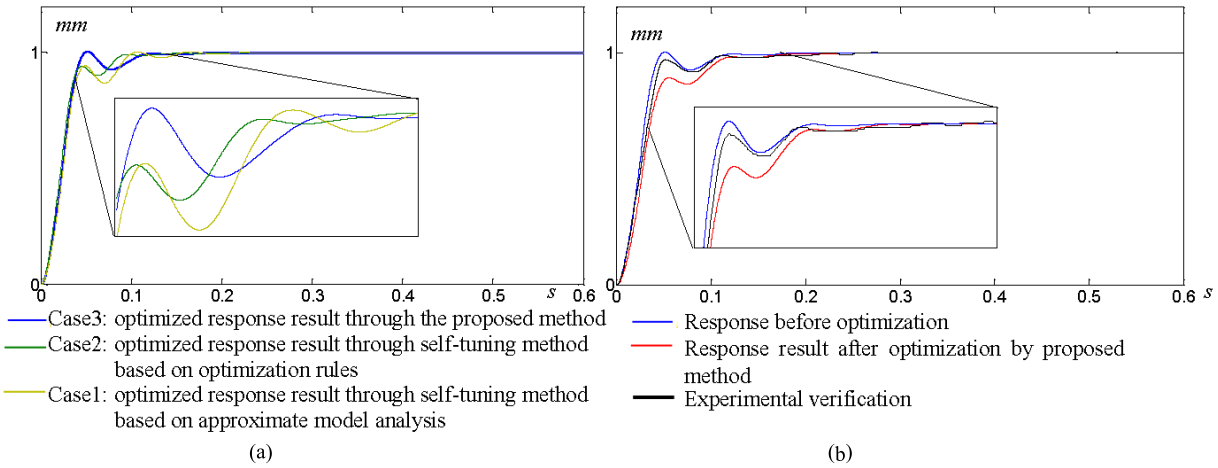

FIGURE 14. Step response curve. (a) Optimized response result through different method. (b) Experience verification.

in Case 3 is best, which has both the optimal response speed and the setting process.

It should be noted that: In Case 1, the value of analytic derivation of servo controller based on the extraction of state space modal characteristics i.e. the global optimization in section 3.1 is adopted. It can inferred obviously that the optimization through analysis derivation based on the approximate model simplifying mechanical transmission into one equivalent rigid body is worse, which involves less the structural flexibility and modal vibration and is clearly incompatible with the actual situation.

In addition, as mentioned above, self-tuning method based on optimization rules often use the initial value of variables are from experience. So Case 2 uses the same optimization conditions as Case 3, such as the same optimization algorithm, etc. but uses random variables as initial values of servo control parameters.

Based on the proposed optimization method of overall dynamic performance and servo parameters of feed drive system under the influence of modal characteristic of mechanical transmission, the step response curves before and after optimization (the red and the blue) are shown in Fig. 14(b). By analysis, it can be obtained that: the rise time and the settling time are 0.089s and 0.104s before optimization; the rise time and the settling time are 0.038s and 0.092s after optimization. It can be known also from the figure that: after the optimization, the dynamic response performance of whole feed drive system is better, and the system has faster response and no overshoot.

The overall dynamic performance and servo control parameters after optimization are tested by experiment with the same control parameters, and in order to compare the simulation and test easily, the step response by test is also shown in Fig. 14(b). By analysis, it can be obtained that: the rise time and the settling time by simulation are 0.038s and 0.092s respectively from the simulation; while the rise time and the settling time by experiment test are 0.042s and 0.094s. Moreover the consistency of curves from experiment and simulation is well.

All these show that shows the reliability and validity of this optimization method of overall dynamic performance and servo parameters considering the modal characteristic influence of mechanical transmission fully is well.

V. CONCLUSIONS

The accurate prediction and research about the dynamic characteristic of machine tool during the design process is essential to develop high performance machines. In this study, we propose the dynamic characteristic prediction and optimization method of ball screw feed drive in machine tool based on modal extraction of state space model. Though the comparison to the former methods, also by the experiment verification, it can be concluded that: based on this proposed method, the dynamic performance and the best motion response characteristics of ball screw feed system can be accurately predicted and determined, which can reduce the cost and time of iterative improvements of the physical prototype in the design process and whole product development cycle.

REFERENCES

[1] M. Postel, O. Özsahin, and Y. Altintas, "High speed tooltip FRF predictions of arbitrary tool-holder combinations based on operational spindle identification," *Int. J. Mach. Tools Manuf.*, vol. 129, pp. 48–60, Jun. 2018.

[2] J.-X. Chena, S.-W. Lina, and X.-L. Zhou, "A comprehensive error analysis method for the geometric error of multi-axis machine tool," *Int. J. Mach. Tools Manuf.*, vol. 106, pp. 56–66, Jul. 2016.

[3] A. Rushworth, D. Axinte, M. Raffles, and S. Cobos-Guzman, "A concept for actuating and controlling a leg of a novel walking parallel kinematic machine tool," *Mechatronics*, vol. 40, pp. 63–77, Dec. 2016.

[4] D. Aslan and Y. Altintas, "On-line chatter detection in milling using drive motor current commands extracted from CNC," *Int. J. Mach. Tools Manuf.*, vol. 132, pp. 64–80, Sep. 2018.

[5] I. Ansoategui and F. J. Campa, "Mechatronics of a ball screw drive using an N degrees of freedom dynamic model," *Int. J. Adv. Manuf. Technol.*, vol. 93, nos. 1–4, pp. 1307–1318, 2017.

[6] C. Li, C. P. Liu, and Z. Wang, "Model reference adaptive modeling method of ball screw feed system," *Appl. Mech. Mater.*, vols. 543–547, pp. 1409–1412, Mar. 2014.
[7] C. Zhang and Y. Chen, "Tracking control of ball screw drives using ADRC and equivalent-error-model-based feedforward control," *IEEE Trans. Ind. Electron.*, vol. 63, no. 12, pp. 7682–7692, Dec. 2016.
[8] V. L. Orekhov, C. S. Knabe, M. A. Hopkins, and D. W. Hong, "An unlumped model for linear series elastic actuators with ball screw drives," in *Proc. IEEE/RSJ Int. Conf. Intell. Robots Syst. (IROS)*, Sep./Oct. 2015, pp. 2224–2230.
[9] H.-W. Huang, M.-S. Tsai, and Y.-C. Huang, "Modeling and elastic deformation compensation of flexural feed drive system," *Int. J. Mach. Tools Manuf.*, vol. 132, pp. 96–112, Sep. 2018.
[10] Y.-Q. Wang and C.-R. Zhang, "Simulation modeling of a ball screw feed drive system," *J. Vib. Shock*, vol. 32, no. 3, pp. 46–49, 2013.
[11] Y. M. Hendrawan, K. R. Simba, and N. Uchiyama, "Iterative learning based trajectory generation for machine tool feed drive systems," *Robot. Comput.-Integr. Manuf.*, vol. 51, pp. 230–237, Jun. 2018.
[12] Z. Lei, T. Wang, G. Wang, and S. Tia, "Hybrid dynamic modeling and analysis of a ball-screw-drive spindle system," *J. Mech. Sci. Technol.*, vol. 31, no. 10, pp. 4611–4618, 2017.
[13] H. Zhang, J. Zhang, H. Liu, T. Liang, and W. Zhao, "Dynamic modeling and analysis of the high-speed ball screw feed system," *Proc. Inst. Mech. Eng. B, J. Eng. Manuf.*, vol. 229, no. 5, pp. 870–877, 2014.
[14] B. He, W. Tang, and J. Cao, "Virtual prototyping-based multibody systems dynamics analysis of offshore crane," *Int. J. Adv. Manuf. Technol.*, vol. 75, nos. 1–4, pp. 161–180, 2014.
[15] Y.-F. Yao, Q. Liu, and W.-J. Wu, "Dynamic simulation of a linear motor feed drive system based on rigid-flexible & electrical-mechanical coupling," *J. Vib. Shock*, vol. 30, no. 1, pp. 191–196, 2011.
[16] Y. Liu, M. Zhang, P. Huo, J. Zhan, and R. Li, "Analyze ball screw feeding system dynamics simulation based on the ADAMS," *Int. J. Res. Eng. Sci.*, vol. 2, no. 10, pp. 1–7, 2014.
[17] C. Deng, G. Yin, H. Fang, and Z. Meng, "Dynamic characteristics optimization for a whole vertical machining center based on the configuration of joint stiffness," *Int. J. Adv. Manuf. Technol.*, vol. 76, nos. 5–8, pp. 1225–1242, 2015.
[18] Y. Shi, X. Zhao, H. Zhang, Y. Nie, and D. Zhang, "A new top-down design method for the stiffness of precision machine tools," *Int. J. Adv. Manuf. Technol.*, vol. 83, nos. 9–12, pp. 1887–1904, 2016.
[19] X. Gao, B. Li, J. Hong, and J. Guo, "Stiffness modeling of machine tools based on machining space analysis," *Int. J. Adv. Manuf. Technol.*, vol. 86, nos. 5–8, pp. 2093–2106, 2016.
[20] D. Tesch, D. Eckhard, and A. S. Bazanella, "Iterative feedback tuning for cascade systems," in *Proc. Eur. Control Conf. (ECC)*, Jun./Jul. 2017, pp. 495–500.
[21] H. Hjalmarsson, "Efficient tuning of linear multivariable controllers using iterative feedback tuning," *Int. J. Adapt. Control Signal Process.*, vol. 13, no. 7, pp. 553–572, 1999.
[22] B. Feng, J. Yang, J. Ren, and D. Zhang, "Control parameters optimization for servo feed system using an improved genetic algorithm," in *Proc. 11th World Congr. Intell. Control Automat.*, Jun./Jul. 2015, pp. 4865–4870.
[23] R. Wang and X. Zhang, "Parameters optimization and experiment of a planar parallel 3-DOF nanopositioning system," *IEEE Trans. Ind. Electron.*, vol. 65, no. 3, pp. 2388–2397, Mar. 2018.
[24] B. Y. Liao, X. M. Zhou, and Z. H. Yin, *Modern Mechanical Dynamics and its Engineering Applications: Modeling, Analysis, Simulation, Modication, Control And optimization*. (in Chinese), Beijing, China: Machinery Ind. Press, 2004
[25] J.-S. Fuh and S.-Y. Chen, "Constraints of the structural modal synthesis," *AIAA J.*, vol. 38, no. 24, pp. 1045–1047, 2015.
[26] K. M. Nittler and R. T. Farouki, "A real-time surface interpolator methodology for precision CNC machining of swept surfaces," *Int. J. Adv. Manuf. Technol.*, vol. 83, nos. 1–4, pp. 561–574, 2016.
[27] Q. Liu *et al.*, "Identification and optimal selection of temperature-sensitive measuring points of thermal error compensation on a heavy-duty machine tool," *Int. J. Adv. Manuf. Technol.*, vol. 85, nos. 1–4, pp. 345–353, 2016.
[28] Y.-P. Shih and C. H. You, "On-machine quasi-3D scanning measurement of bevel gears on a five-axis CNC machine," *J. Chin. Inst. Eng.*, vol. 40, no. 3, pp. 207–218, 2017.
[29] *User Manual of SINUMERIK 840D SL/840Di SL/840D/840Di/810D functions [Z]*, SIEMENS IA&DT, Erlangen, Germany, 2006.
[30] *User Manual of SIMODRIVE 611 Digital Drive Converters Configuration [Z]*, SIEMENS IA&DT, Erlangen, Germany, 2007.
[31] H. Groß, J. Hamann, and G. Wiegärtner, *Elektrische Vorschubantriebe in der Automatisierungstechnik: Grundlagen, Berechnung, Bemessung*. Beijing, China: China Machine Press, 2000.
[32] M. F. Zaeh and M. Hennauer, "Prediction of the dynamic behaviour of machine tools during the design process using mechatronic simulation models based on finite element analysis," *Prod. Eng.*, vol. 5, no. 3, pp. 315–320, 2011.
[33] X. Xu, T. Tao, G. Jiang, X. Huang, R. Liu, and L. Liu, "Monitoring and source tracing of machining error based on built-in sensor signal," *Procedia CIRP*, vol. 41, pp. 729–734, 2016. [Online]. Available: https://www.infona.pl/resource/bwmeta1.element.elsevier-3cd8951b-09d0-37a0-8777-075cd8f437f0/tab/summary
[34] Y. Yamada and Y. Kakinuma, "Sensorless cutting force estimation for full-closed controlled ball-screw-driven stage," *Int. J. Adv. Manuf. Technol.*, vol. 87, nos. 9–12, pp. 3337–3348, 2016.
[35] Y. Kakinuma and S. Nagakari, "Sensor-less micro-tool contact detection for ultra-precision machine tools utilizing the disturbance observer technique," *CIRP Ann.*, vol. 66, no. 1, pp. 385–388, 2017.
[36] K. P. Yu and J. X. Zou, *Structural Dynamics*. Harbin, China: Harbin Univ. Technol. Press, (in Chinese), 2015.
[37] H. Hao, *Principle of Automatic Control*. (in Chinese), Xi'an, China: Xi'an Univ. of Electronic Science and Technology Press, 2016.

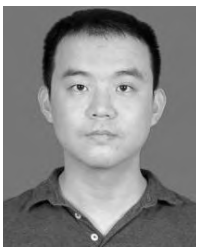

YANG YONG received the B.S. degree in mechanical engineering and automation from Hehai University, Jiangsu, China, in 2007, the M.S. degree in weapon launching theory and technology from the Nanjing University of Technology, Jiangsu, in 2009, and the Ph.D. degree in mechanical manufacturing and automation from Tongji University, Shanghai, China, in 2015. He is currently a Lecturer with the College of Mechanical Engineering, Suzhou University of Science and Technology. His main research interests include the dynamic performance of ball screw feed drive of NC machine tools, structural dynamics of machine tools, and so on.

ZHANG WEI-MIN received the B.S., M.S., Ph.D. degrees in mechanical manufacturing and automation from Tongji University, Shanghai, China. He is the Deputy Director of the Institute of Modern Manufacturing Technology, Tongji University, where he is the Director of the Production System Research Department, Sino-German College. He is also a Professor and the Doctor's Supervisor with Tongji University. He is mainly engaged in the teaching and research of mechanical design and manufacturing and automation. His research direction is manufacturing systems and automation, digital manufacturing technology, modular manufacturing, and control technology.

ZHU QI-XIN received the Ph.D. degree in control theory and control engineering from the School of Automation, Nanjing University of Aeronautics and Astronautics, Jiangsu, China. He is a Professor and a Master's Supervisor with the School of Mechanical Engineering, Suzhou University of Science and Technology, Jiangsu. He is a member of the Standing Committee of the International Union of Aquatic Robots, the Professional Committee of Modeling and Simulating Intelligent Object System of the Chinese Society of Systems Simulation, and the Professional Committee of Cloud Control and Decision Making of the Chinese Society of Command and Control. He is a Reviewer of more than 20 international authoritative journals, such as *Automatica*, the IEEE TRANSACTIONS ON INDUSTRIAL ELECTRONICS, the IEEE TRANSACTIONS ON CYBERNETICS, and the *International Journal of Control*. He is mainly engaged in the research of networked control systems, electromechanical servo systems, robots, advanced control theory and application, and the automation of construction equipment.

JIANG QUAN-SHENG received the Ph.D. degree in mechanical manufacturing and automation from Southeast University, Jiangsu, China, in 2009. He is an Associate Professor and a Master's Supervisor with the School of Mechanical Engineering, Suzhou University of Science and Technology, Jiangsu. He is mainly engaged in intelligent equipment condition monitoring and fault diagnosis research work, such as: 1) complex mechanical and electrical equipment non-linear fault diagnosis method; 2) intelligent manufacturing systems and equipment technology; and 3) robotics and automation technology.